May 1994

Electronic structure and Curie temperature of $YFe_{12-x}Mo_xN_y$ compounds

A.S. Fernando
University of Nebraska - Lincoln

J.P. Woods
University of Nebraska - Lincoln

Sitaram Jaswal
University of Nebraska, sjaswal1@unl.edu

D. Welipitiya
University of Nebraska - Lincoln

B.M. Patterson
University of Nebraska - Lincoln

See next page for additional authors

Electronic structure and Curie temperature of $YFe_{12-x}Mo_xN_y$ compounds

A. S. Fernando, J. P. Woods, S. S. Jaswal, D. Welipitiya, B. M. Patterson, and D. J. Sellmyer
Behlen Laboratory of Physics and Center for Materials Research and Analysis, University of Nebraska, Lincoln, Nebraska 68588-0111

The electronic structures of $YFe_{12-x}Mo_xN_y$, where $x=1.0$, 2.0 and $y=0$, 0.7, have been studied with photoemission and spin-polarized calculations. The peak near the Fermi level in the energy distribution curves (EDC) becomes successively broader with larger Mo concentration. The features in the calculated density of state at 1.3 and 2.7 eV are not readily seen in the EDC, and this may be due to lifetime effects in these compounds. Finally, changes in Curie temperature (T_c) with the change of N or Mo concentration are compared with prediction of the theory of Mohn and Wohlfarth. Reasonable agreement is obtained in the N case but not in the Mo case, the latter most likely due to hybridization of Fe and Mo d bands.

I. INTRODUCTION

Superior permanent-magnet materials require large saturation magnetization, high Curie temperature (T_c), and large uniaxial anisotropy. The best permanent magnetic materials are rare-earth(R)–transition-metal(T) compounds. The transition metals Fe and Co have large magnetic moments and high Curie temperatures, and the R-T compounds often have large uniaxial magnetic anisotropies. The Fe-rich ternary compound $Nd_2Fe_{14}B$ has an energy product as high as 45 MgOe,[1–4] but the relatively low T_c (≈300 °C) of this material limits its application. Permanent-magnet materials research is currently investigating other Fe-rich R-T compounds. The RT_{12} body-centered-tetragonal compound with the $ThMn_{12}$ structure does not exist in the binary phase, but the structure is stabilized with the partial substitution of a nonmagnetic element (M) for Fe. The compounds $RFe_{12-x}M_x$ with M=Ti, V, Cr, Mo, W, and Si have been fabricated and their magnetic properties examined.[5] The addition of interstitial nitrogen increases the Curie temperature of the materials and the magnetic anisotropy may change.[6] For example, T_c of $NdFe_{11}Ti$ increases by 30% upon nitriding and the magnetic anisotropy changes from in-plane to uniaxial.[7]

The magnetic properties of the compound $YFe_{12-x}Mo_x$ with $x=0.5$, 1, 2, 4 have been published.[8] T_c decreases with increased Mo concentration, and increases with nitriding; the volume increases both with increased Mo and N concentration. The Mo atoms substitute for Fe atoms on the (i) site with the largest magnetic moment.[9]

The magnetic properties of the compounds are determined by the electronic configuration, and the increase in T_c of Y_2Fe_{17} (Ref. 10) and $NdFe_{11}Ti$ (Ref. 11) upon nitriding has been modeled using electronic structure calculations and the spin-fluctuation theory of Mohn and Wohlfarth.[12] Briefly,

$$(T_c)_{M-W}=CM_0^2/\chi_0, \tag{1}$$

where M_0 is the magnetic moment per Fe site, χ_0 is the enhanced susceptibility, and C is a constant. In earlier work the electronic structure of $Sm_2Fe_{17}N_y$ with $y=0$ and $y=2.6$ has been measured with photoelectron spectroscopy (PES), and a decrease in the density of state (DOS) at E_F is observed as nitrogen is added which agrees with the calculated DOS.[13] In this paper the electronic structure of $YFe_{12-x}Mo_xN_y$ with $x=1$, 2, and $y=0$, 0.7 is examined with PES, and the calculated partial DOS for Fe, Y, and Mo in $YFe_{11}Mo$ are given. Comparison with the expected changes in T_c are presented.

II. EXPERIMENTAL PROCEDURE

Bulk samples of $YFe_{12-x}Mo_x$ with $x=1$, 2 were prepared by arc melting the elemental constituents in a water-cooled copper boat in flowing-argon gas atmosphere. All the starting elements used were at least 99.98% purity. The alloys were melted several times to insure homogeneity. The samples were wrapped separately in Ta foils and heat treated in vacuum below 3×10^{-6} Torr at 1100 °C for about 50 h,[8] and subsequently quenched in water. X-ray diffraction measurements on powder samples using Cu K_α radiation showed that the samples were composed of primarily the $ThMn_{12}$ structure with a small amount of α-Fe. The magnetization of the samples was measured at 5 and 300 K with superconducting quantum interference device (SQUID) and alternating force gradient magnetometers, respectively, and the saturation magnetic moments agree with published results.[8]

The arc-melted buttons were spark cut into discs ~1 mm thick to expose an interior surface which was then polished to provide an optically smooth surface for PES measurements. The samples were mounted on a tungsten sample manipulator using 0.25-mm-diam tantalum wires in an ultrahigh vacuum chamber with a base pressure of 2×10^{-10} Torr. Each sample was cleaned *in situ* with several cycles of 2 keV Ar sputtering and subsequent annealing at 350 °C. Auger electron spectroscopy (AES) was employed to monitor surface cleanliness and to estimate the nitrogen concentration. After cleaning the sample, nitrogen was introduced by ion implantation with a kinetic energy of 2 keV and a current density of 25 μA/cm^2 for 10 min.[13] The subsequent nitrogen concentration was measured with AES as $y=8.3\pm0.8$. The samples were then radiantly heated to 350 °C for several minutes to promote nitrogen diffusion from the nitrogen-rich surface into the subsurface region. The nitrogen-rich surface layer was subsequently removed with Ar sputtering to expose the subsurface nitride and the resulting surface nitrogen concentration measured with AES was $y\approx0.7\pm0.3$. Quantitatively, the nitrogen concentration per formula unit of 0.7 at the sur-

 0021-8979/94/75(10)/6303/3/$6.00

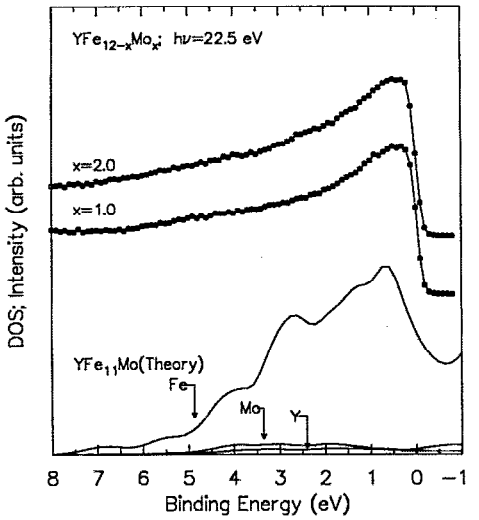

FIG. 1. Calculated partial spin-polarized DOS of Fe, Mo, and Y in $YFe_{11}Mo$ and experimental energy distribution curves (EDC) for clean $YFe_{12-x}Mo_x$ ($x=1.0$, 2.0). The EDCs are normalized to the area under the EDC curves between 0 and 3.5 eV and shifted vertically. The zero on the binding energy axis refers to the Fermi energy (E_F).

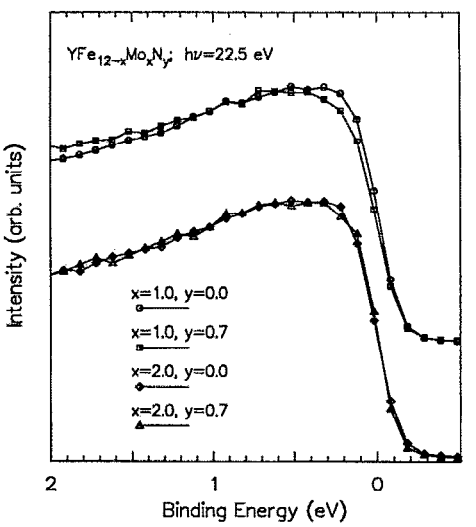

FIG. 2. Expand view of the experimental EDCs of $YFe_{11}MoN_y$ for $y=0.0$, $y=0.7$ (upper two curves) and of $YFe_{10}Mo_2N_y$ for $y=0.0$, $y=0.7$ (lower two curves). The zero on the binding energy axis corresponds to the Fermi energy.

face of 1:12 compounds here and previously published[11] is in agreement with published bulk values[7] and supports the assertion that the bulk atomic structure is present up to the surface which is probed by AES and PES. The electronic structure was measured with PES experiments which were performed at the Synchrotron Radiation Center in Wisconsin. The photoelectron energy distribution curves (EDC) presented were obtained with a photon energy of 22.5 eV and a total energy resolution of 0.14 eV.

III. ELECTRONIC STRUCTURE

The EDCs from the Ar-sputter-cleaned and annealed $YFe_{12-x}Mo_x$ samples with bulk values of $x=1.0$, 2.0, and the calculated partial DOS for each element in $YFe_{11}Mo$ are shown in Fig. 1. The EDC curves have been normalized to the same areas between 0 and 3.5 eV binding energy and the baseline for each EDC is shifted vertically. The DOS are determined with self-consistent spin-polarized calculations using linear-muffin-tin orbitals in the scalar relativistic approximation.[14] A supercell consisting of four formula units was used to simulate the ternary compound with correct stoichiometry. The total DOS (not shown) is the sum of the three partial DOS curves, and the total DOS is dominated by the Fe DOS, due to the large atomic percentage (85%) of Fe in the compound. The present Fe DOS is substantially different from Fe DOS in $NdFe_{11}Ti$ compounds[11] and the difference is due to the strong hybridization with Mo.

The EDCs are comparable to the calculated DOS with a 1–2 eV wide peak at the Fermi energy. The features in the calculated DOS at 1.3 and 2.7 eV are not readily discernible in the EDC, and this may be due to lifetime effects in these compounds.[15]

The change in EDCs at E_F after nitriding $YFe_{11}Mo$ and $YFe_{10}Mo_2$ compounds are shown in Fig. 2. The $YFe_{11}Mo$ sample (upper two curves) shows a significant decrease in EDC at E_F upon nitriding; the $YFe_{10}Mo_2$ sample (lower two curves) does not show any significant change in EDC at E_F upon nitriding. The comparison of EDCs for $x=1$ and $x=2$ without nitrogen (upper two curves) and with nitrogen (lower two curves) are shown in Fig. 3. The EDCs at E_F for $YFe_{11}Mo$ and $YFe_{10}Mo_2$ show no significant change; the nitrided samples $YFe_{11}MoN_{0.7}$ and $YFe_{10}Mo_2N_{0.7}$ show a slight increase in EDC at E_F as the Mo:Fe ratio is increased.

In previous experiments on 1:12 and 2:17 compounds[11,13] the change in the EDCs at E_F was compared

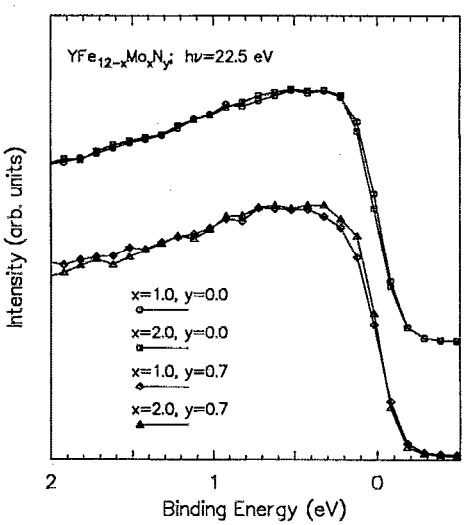

FIG. 3. Expand view of EDCs of unnitrided (upper two curves) and nitrided (lower two curves) samples of $YFe_{12-x}Mo_x$ ($x=1.0$, 2.0). The zero on the binding energy axis refers to the Fermi energy.

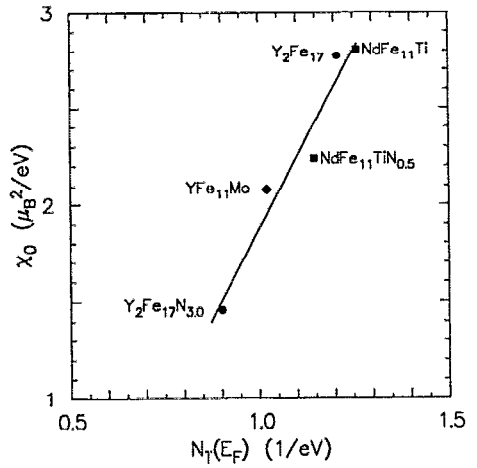

FIG. 4. Calculated χ_0 vs calculated $N_T(E_F)$ for the samples listed.

to the calculated[10,16] total DOS, $N_T(E_F)=N_\uparrow(E_F)+N_\downarrow(E_F)$, where $N_\uparrow(E_F)$ and $N_\downarrow(E_F)$ are the up- and down-spin DOS at the Fermi level, respectively. The calculated DOS, Stoner parameter, and magnetic moments used with Mohn and Wohlfarth theory predict a change in T_c upon nitrogenation which agrees very well with measured change in T_c. In the present experiment the calculated DOS is available only for the $YFe_{11}Mo$ compound, and a comparison of changes in $N_T(E_F)$ as the nitrogen concentration or the Fe:Mo ratio changed is not possible.

In order to compare changes in the measured electronic structure with changes in the magnetic properties (T_c and M_0), a dependence of χ_0 on $N_T(E_F)$ is required. Calculated values of χ_0 for listed samples, where $\chi_0^{-1}=[1/N_\uparrow(E_F)+1/N_\downarrow(E_F)-2I]/4\mu_B^2$ are plotted as a function of $N_T(E_F)$ in Fig. 4. There is a linear dependence between χ_0 and $N_T(E_F)$ in the small range of $N_T(E_F)$ for the 1:12 and 2:17 Fe-based compounds considered. With this plot, the electronic structure is related to T_c and M_0 as $M_0^2/T_c \propto \chi_0 = AN_T(E_F)+B$, where A and B are constants and $B/A=-0.48$ eV^{-1}. Upon alloying with either N or Mo, the new value of T_c (T_c') can be related through Eq. (1) to the measured changes in magnetization and electronic structure by

$$(T_c'/T_c)_{M-W}=(M_0'^2/M_0^2)(\chi_0/\chi_0'), \tag{2}$$

where χ_0/χ_0' is given by $[N_T(E_F)-0.48]/[N_T'(E_F)-0.48]$. The values of $N_T(E_F)$ are obtained from the experimental EDC curves. The ratio $(T_c'/T_c)_{\rm exp}$ measured directly, and $(T_c'/T_c)_{M\text{-}W}$ are shown in Table I.

As shown in Table I, these two values agree fairly well when nitrogen is added to the two parent compounds. However, when the nitrogen concentration is held fixed and the Fe:Mo ratio is varied, there is a large disagreement between these two values. The disagreement is due to the fact that substitution of Mo for Fe in going from $YFe_{11}Mo$ to $YFe_{10}Mo_2$ lowers the Fe concentration and causes a strong hybridization of the Fe and Mo d bands thus changing the proportionality constant in Eq. (1).

TABLE I. Calculated values of $(T_c'/T_c)_{M-W}$ and $(T_c'/T_c)_{\rm exp}$ for $YFe_{12-x}Mo_xN_y$ samples.

x,y	$(M_0'/M_0)^2$ [a]	(χ_0/χ_0') [b]	$(T_c'/T_c)_{M-W}$ ±8%	$(T_c'/T_c)_{\rm exp}$ [a]
1,0.0 1,0.7	1.10	1.24	1.36	1.41
2,0.0 2,0.7	1.59	0.98	1.56	1.48
1,0.0 2,0.0	0.44	0.95	0.42	0.68
1,0.7 2,0.7	0.62	0.75	0.46	0.72

[a]Reference 8.
[b]Based on experimental $N_T(E_F)$ values.

IV. CONCLUSIONS

PES experiments probing the electronic structure agree approximately with the calculated DOS. The samples with fixed Mo concentration follow the Curie-temperature theory of Mohn and Wohlfarth upon nitriding. However, the theory does not correctly predict changes in T_c on alloying with Mo. The reason for this appear to be that nitrogen goes into the lattice interstitially and mainly expands the lattice, whereas Mo substitution for Fe causes a significant change in the electronic structure of the material.

ACKNOWLEDGMENTS

We are grateful to the United States Department of Energy for support under Grant No. DE-FG02-86ER45262, Nebraska Energy Office and to the Cornell National Supercomputing Facility which is funded by the National Science Foundation. The authors thank the staff of the Synchrotron Radiation Center at the University of Wisconsin.

[1] M. Sagawa, S. Fujimura, N. Togawa, and Y. Matsuura, J. Appl. Phys. **55**, 2083 (1984).
[2] G. C. Hadjipanayis, R. C. Hazeton, and K. R. Lawless, Appl. Phys. Lett. **43**, 797 (1983).
[3] J. J. Croat, J. F. Herbst, R. W. Lee, and F. E. Pinkerton, Appl. Phys. Lett. **44**, 148 (1984).
[4] K. S. V. L. Narasimhan, in *Proceedings of the 8th International Workshop on Rare-Earth Magnets and their Applications*, edited by K. J. Strnat (University of Dayton, Dayton, OH, 1985), p. 459.
[5] D. B. de Mooij and K. H. J. Buschow, J. Less Common Met. **136**, 207 (1988).
[6] J. M. D. Coey, H. Sun, and D. P. F. Hurley, J. Magn. Magn. Mater. **101**, 310 (1991).
[7] Y.-C. Yang, X.-D. Zhang, L.-S. Kong, and Q. Pan, Solid State Commun. **78**, 317 (1991).
[8] H. Sun, M. Akayama, K. Tatami, and H. Fujii, Physica B **183**, 33 (1993).
[9] C. J. M. Denissen, R. Coehoorn, and K. H. J. Buschow, J. Magn. Magn. Mater. **87**, 51 (1990).
[10] S. S. Jaswal, W. B. Yelon, G. C. Hadjipanayis, Y. Z. Wang, and D. J. Sellmyer, Phys. Rev. Lett. **67**, 644 (1991).
[11] A. S. Fernando, J. P. Woods, S. S. Jaswal, B. M. Patterson, D. Welipitiya, A. S. Nazareth, and D. J. Sellmyer, J. Appl. Phys. **73**, 6919 (1993).
[12] P. Mohn and E. P. Wohlfarth, J. Phys. F **17**, 2421 (1987).
[13] J. P. Woods, A. S. Fernando, S. S. Jaswal, B. M. Patterson, D. Welipitiya, and D. J. Sellmyer, J. Appl. Phys. **73**, 6913 (1993).
[14] H. L. Skriver, *The LMTO Method*, Vol. 41 of the Springer Series in Solid State Sciences (Springer, New York, 1984).
[15] M. M. Steiner, R. C. Albers, L. J. Sham, Phys. Rev. B **45**, 13272 (1992).
[16] S. S. Jaswal, Phys. Rev. B **48**, 6156 (1993).